BIOCHEMISTRY
including biophysical chemistry & molecular biology

ARTICLE

pubs.acs.org/biochemistry

The Role of Conserved Glu Residue on Cyclotide Stability and Activity: A Structural and Functional Study of Kalata B12, a Naturally Occurring Glu to Asp Mutant

Conan K. L. Wang, Richard J. Clark, Peta J. Harvey, K. Johan Rosengren, Masa Cemazar, and David J. Craik*

Institute for Molecular Bioscience, The University of Queensland, Brisbane, Queensland, 4072, Australia

ABSTRACT: Cyclotides are a family of plant defense proteins with a unique cyclic backbone and cystine knot. Their remarkable stability under harsh thermal, enzymatic, and chemical conditions, combined with their range of bioactivities, including anti-HIV activity, underpins their potential as protein drug scaffolds. The vast majority of cyclotides possess a conserved glutamate residue in loop 1 of the sequence that is involved in a structurally important network of hydrogen bonds to an adjacent loop (loop 3). A single native cyclotide sequence, kalata B12, has been discovered that has an aspartic acid in this otherwise conserved position. Previous studies have determined that methylation of the glutamate or substitution with alanine abolishes the membrane disrupting activity that is characteristic of the family. To further understand the role of this conserved structural feature, we studied the folding, structure, stability, and activity of the natural aspartic acid variant kalata B12 and compared it to the prototypical cyclotide kalata B1, along with its glutamate to alanine or aspartate mutants. We show that the overall fold of kalata B12 is similar to the structure of other cyclotides, confirming that the cyclotide framework is robust and tolerant to substitution, although the structure appears to be more flexible than other cyclotides. Modification of the glutamate in kalata B1 or replacing the aspartate in kalata B12 with a glutamate reduces the efficiency of oxidative folding relative to the native peptides. The bioactivity of all modified glutamate cyclotides is abolished, suggesting an important functional role of this conserved residue. Overall, this study shows that the presence of a glutamic acid in loop 1 of the cyclotides improves stability and is essential for the membrane disrupting activity of cyclotides.

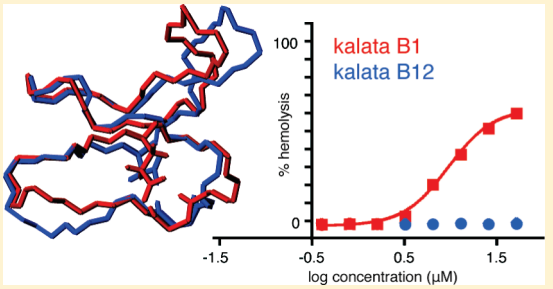

Cyclotides[1] are a family of topologically unique proteins that have a role in plant defense[2−5] and display a range of interesting bioactivities, including uterotonic,[6] anti-HIV,[7,8] antimicrobial,[9] cytotoxic,[10] and neurotensin antagonistic[11] activities. Their natural function as plant defense agents was proposed after it was found that insect larvae from two common plant pests, *Helicoverpa punctigera* and *H. armigera,* showed severely retarded growth after being fed a diet that contained cyclotides.[2,4] Cyclotides have also been reported to have molluscicidal activity[12] against Golden Apple snail, a pest of rice crops in South-East Asia. The ability to deliver their activity in the environments of insect and mollusc guts demands a high degree of stability, and cyclotides have been shown to be stable when subjected to harsh thermal, chemical, and enzymatic conditions.[13] Their stability is important for their natural pesticidal functions, and it also allows pharmaceutically active peptide sequences to be grafted onto their rigid framework, making them potential drug scaffolds.[14]

The stability of cyclotides is attributed to their unique topology. They are distinguished by a cyclic cystine knot (CCK) motif, which is characterized by a circular backbone and a three-disulfide knotted core.[1] Two of the disulfide bonds form a ring with the intervening backbone sequences, through which the third disulfide bond penetrates.[15] Figure 1 shows the alignment of a selection of cyclotide sequences and the disulfide bond connectivity. The backbone sequences between consecutive cysteine residues are termed loops, with loops 1 and 4 forming part of the embedded ring that makes up the cystine knot. The stabilizing features of the macrocyclic backbone and cystine knot are complemented by a network of hydrogen bonds that further stabilize the structure.

Cyclotides are the largest family of circular proteins, currently comprising more than 160 members, and it is predicted that many thousands await discovery.[16,17] Although the first cyclotide discovered, kalata B1 (kB1), was found in *Oldenlandia affinis*,[18] a member of the Rubiaceae plant family, the majority of known cyclotides have been discovered in the Violaceae plant family. Cyclotides are divided mainly into two subfamilies, Möbius and bracelet, depending on the presence or absence, respectively, of a *cis*-Pro peptide bond in loop 5. In general, cyclotide sequences show a high degree of sequence diversity. Except for the six requisite cysteine residues, each position can accommodate amino acid substitutions. The most highly conserved non-cysteine residue is a Glu residue in loop 1, which has been found to be both structurally and functionally important. This residue contributes to cyclotide stability by forming a hydrogen bond network with two other residues in loop 3.[19] The Glu also

Received: March 20, 2011
Published: April 05, 2011

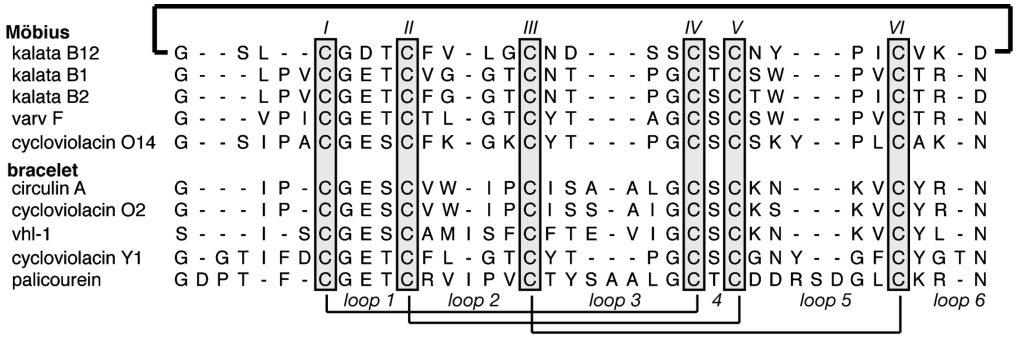

Figure 1. Sequence alignment of selected cyclotides. Cyclotides have six cysteines (I—VI) and six loops made up of the backbone segments between successive cysteines. The disulfide connectivity is shown at the bottom of the alignment, and a thick line connecting the two ends of the sequence at the top depicts the circular backbone. Cyclotides are divided into two subfamilies, Möbius and bracelet, depending on the presence or absence, respectively, of a *cis*-Pro peptide bond in loop 5. Kalata B12 belongs to the Möbius subfamily because it has a *cis*-Pro in loop 5 and is the only naturally occurring cyclotide discovered so far that does not have a Glu in loop 1.

regulates the activity of the cyclotides because an Ala mutant of kB1, E7A-kB1, which has the Glu replaced with an Ala residue, did not have insecticidal or hemolytic activity.[20] In addition, a derivative of cycloviolacin O2, a bracelet cyclotide in which the Glu was chemically modified (methylated), showed a 48-fold decrease in cytotoxic activity relative to its native form.[21]

Recently, a study[22] of cyclotides from *O. affinis* reported the discovery of kalata B12 (kB12), a Möbius cyclotide, which is the only naturally occurring cyclotide to have an Asp in the position of the highly conserved Glu in loop 1. Therefore, it was of interest to characterize kB12 to determine the effect of the Glu to Asp substitution on structure and function. In this paper, we reveal the solution structure of kB12, examine its stability (against enzymes, acid and high temperature), and assess its activity using a hemolytic assay. We compare the results with the prototypical Möbius cyclotide, kB1, and with two synthetic mutants of kB1, E7A-kB1 and E7D-kB1, to study the significance of the Glu residue. This study shows that the presence of a glutamic acid in loop 1 of the cyclotides improves stability and is involved in the membrane disrupting activity of cyclotides.

■ MATERIALS AND METHODS

Peptide Synthesis and Purification. Boc-based solid phase peptide synthesis of kB12 and E7A-kB1 was carried out using a microwave-assisted method described previously,[23] whereas E7D-kB1 and D6E-kB12 were synthesized by manual Boc-based assembly. A thioester based linker was used to facilitate the cyclization via an intramolecular native chemical ligation reaction after peptide cleavage from the resin.[24] Hydrogen fluoride cleavage was conducted on the deprotected resin following standard protocols (0 °C, 90 min, 90% HF/8% *p*-cresol/2% *p*-thiocresol). Crude cleavage products were purified by RP C_{18} HPLC (1%/min gradient of 90% acetonitrile/10% water/0.05% trifluoroacetic acid) to give linear, reduced, C-terminally thioester capped peptides. Peptides were cyclized and oxidized overnight using a range of conditions to optimize folding. Final conditions were 0.1 M NH_4HCO_3 at pH 8.5, containing 25% 2-propanol and glutathione (2 mM reduced) for kB12, 50% 2-propanol for E7A-kB1, and 50% 2-propanol and glutathione (2 mM reduced/0.4 mM oxidized) for E7D-KB1. D6E-kB12 did not fold under any tested conditions. The oxidized peptides were purified by chromatography as above. Purity of fractions was assessed by electrospray ionization-mass spectrometry (ESI-MS) and analytical HPLC using the same gradient and solvent as described above. Native kB1 was extracted from *O. affinis* using a previously described protocol.[2] Briefly, this involves an initial separation step where ground plant material is placed in 1:1 dichloromethane/methanol overnight, followed by repeated rounds of RP C_{18} HPLC.

NMR Spectroscopy. kB12 and E7D-kB1 were dissolved in 90% H_2O/10% D_2O or 100% D2O and Bruker Avance 500, 600, or 900 MHz NMR spectrometers were used to record spectra at either pH 3.0 or 5.0 in the temperature range 283—313 K. All spectra were recorded in phase-sensitive mode using time-proportional phase incrementation.[25] Two-dimensional experiments obtained included a TOCSY[26] with 80 ms mixing time, NOESY[27] with 200 ms mixing time, and E-COSY[28] in 100% D_2O. Water suppression was achieved by using a modified WATERGATE sequence.[29] Spectra were acquired with 4096 data points in the F2 and 512 increments in the F1 dimension. The F1 and F2 dimensions were multiplied by a sine-squared function before Fourier transformation. Chemical shifts were internally referenced to sodium 2,2-dimethyl-2-silapentane-5-sulfonate.

To measure the temperature dependence of the amide chemical shifts, 1D and TOCSY spectra were recorded in steps of 10 K, from 283 to 313 K. The chemical shift movements were documented and fitted to a linear function. Temperature coefficients for kB12 and E7D-kB1 were measured both at pH 3.0 and 5.0.

Structure Determination of kalata B12. Distance restraints were derived from cross-peaks in NOESY spectra recorded with a mixing time of 200 ms at 298 K. Spectra were analyzed with the program SPARKY (http://www.cgl.ucsf.edu/home/sparky/). Backbone dihedral angle restraints were derived from $^3J_{HNH\alpha}$ coupling constants measured from splitting of peaks in a 1D spectrum, while χ^1 dihedral angles were derived from $^3J_{H\alpha H\beta}$ coupling constants from E-COSY spectrum together with NOE intensities. After initial structure calculations were performed using CYANA, hydrogen bond restraints for slowly exchanging amides were added.

In total, 277 distance restraints comprising 95 sequential, 47 nonsequential restraints, and 135 intraresidue restraints were determined from NOESY spectra; 15 dihedral angle restraints (11 ϕ and 4 χ^1) were derived based on coupling constants from DQF-COSY and E-COSY spectra; and slowly exchanging amides, detected >16 h after dissolution of the sample in D_2O,

were used to derived upper limit distance restraints for nine hydrogen bonds.

Final sets of 50 structures were calculated using a torsion angle simulated annealing protocol within CNS[30] and further refined in a water shell. The structures were analyzed with MOLMOL[31] and PROCHECK.[32] For the 20 lowest energy structures, 72.2% of the residues were in the most favored, 27.2% in the additionally allowed, and 0.7% in the generously allowed regions of the Ramachandran plot.

Molecular Dynamics. The lowest energy NMR structures of kB1[19] and kB12, which was solved in this study, were used as the starting structures for molecular dynamics simulations. The system topologies were obtained with the AMBER LEAP module and modeled with the all-atoms AMBER ff99 force field. The proteins were immersed in square boxes filled with TIP3P water molecules, imposing a minimal distance between the solute and the box walls of 12.0 Å.

Optimization and relaxation of solvent were performed, starting with 1000 steps of energy minimization where restraints were placed on atom positions with a weight of 2 kcal $(mol \cdot Å)^{-1}$. The restraints were maintained to a target temperature of 300 K during heating (50 000 steps of 1 fs), which was followed by density equilibration at a constant pressure of 1 bar (50 000 steps of 1 fs). An equilibration period (500 000 steps of 1 fs; 2 bar) was performed before starting the productions runs. The atomic positions were saved every 500 steps (0.5 ps) for the analysis. The system was simulated under periodic boundary conditions, using a cutoff radius of 8.0 Å for the nonbonded interactions. The electrostatic interactions were calculated with the particle mesh Ewald method. The SHAKE algorithm was used to constrain all bond lengths involving hydrogen atoms. The hydrogen bond occupancy was calculated using the 'ptraj' module of AMBER.

Stability Assay. The basic protocol for enzymatic digests and acid hydrolysis assays have been described previously.[13] Performed in triplicate, these assays were modified slightly with a lower starting concentration of peptide. For the enzyme digest assay, 0.5 mg/mL solutions of kB1 and kB12 were prepared in 100 mM ammonium bicarbonate buffer (pH 8.1). Chymotrypsin was added at a substrate-to-enzyme ratio of 50:1 and the digest was carried out at 37 °C with aliquots taken at set times up to 24 h. Melittin was used as a control to ensure that the enzyme was active. Acid hydrolysis reactions (0.5 mg/mL peptide solution in 0.5 M HCl) were performed at 37 °C. Aliquots were drawn at intervals up to 24 h and immediately diluted 100-fold with water containing NaOH to neutralize the acid. Samples were analyzed on an Agilent Series 1100 HPLC. The amount of remaining peptide at each time point was measured by analysis of the peak intensity and expressed as a percentage of the peak intensity at time point 0. Thermal stability of kB12 was assessed by monitoring the quality of 1D NMR spectra in water at pH 5.0 on cycling from 25 to 80 °C and back to 25 °C.

Hemolytic Assay. Stock solutions of kB1, E7A-kB1, E7D-KB1, and kB12 were prepared and standardized using UV spectroscopy (ε_{280} = 5875 cm^{-1} M^{-1} for kB1, E7A-kB1, and E7D-kB1; ε_{280} = 1865 cm^{-1} M^{-1} for kB12) at 350 μM then serially diluted in triplicate. Human erythrocytes were washed repeatedly and centrifuged in phosphate buffered saline (pH 7.4) to remove serum contaminants. A 0.25% v/v stock solution was prepared from the cell pellet and 100 μL of this stock was added to each diluted peptide solution aliquot and then incubated at 37 °C for 1 h. After centrifugation of intact cells, the percentage of hemolysis of the supernatant was measured by visual absorption spectroscopy (λ = 415 nm).

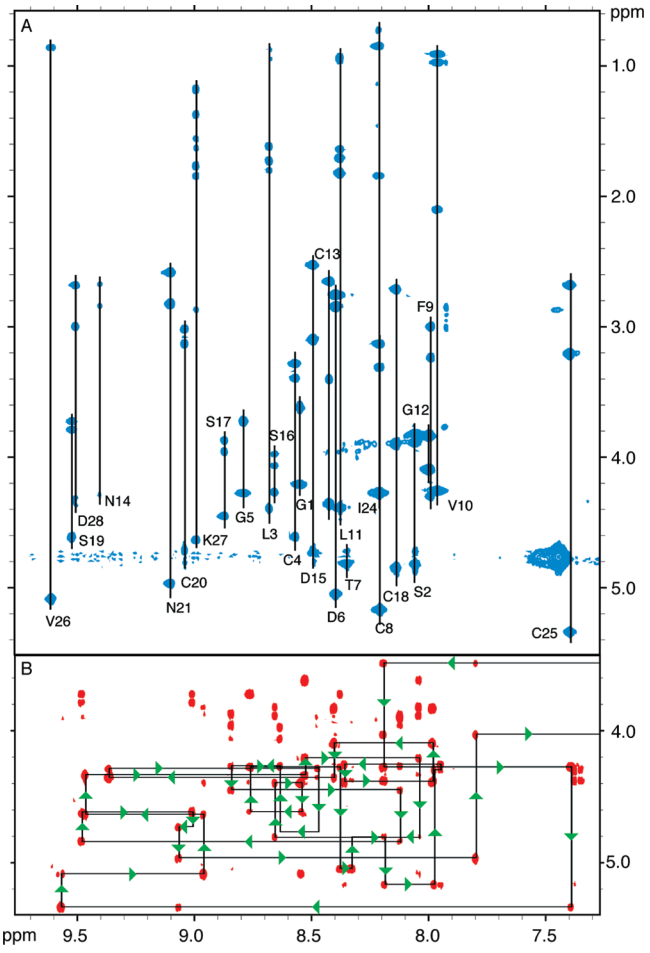

Figure 2. TOCSY and NOESY spectra of kalata B12. Fingerprint region of a 80 ms TOCSY spectrum (panel A) and a 200 ms NOESY spectrum (panel B) in 90% H_2O and 10% D_2O at 298 K and pH 5.0. Spin systems are shown in the TOCSY spectrum and the sequential connectivities in the NOESY spectrum. The one-letter code for the amino acids as well as the residue number is used for the sequence assignments.

RESULTS

Synthesis. Boc-based solid phase peptide chemistry was used to synthesize kB12, D6E-kB12, E7A-kB1, and E7D-kB1. The cyclization was achieved using an intramolecular form[33,34] of native chemical ligation[35] that required the linear precursor protein to have a Cys at the N-terminus. kB12 was cyclized and oxidized at pH 8.5 in a NH_4HCO_3 containing 25% 2-propanol and 2 mM reduced glutathione after cleavage from the resin and purification. Variations of the folding buffer were tested, including different concentrations of 2-propanol and reduced glutathione; the addition of oxidized glutathione, EDTA, DMSO, and guanidine-HCl; replacement of reduced glutathione with cysteine; and varying the incubation time. However, the best yield obtained was 7%. In comparison, kB1 has a reported yield of 28% under similar folding conditions of 1:1 NH_4HCO_3/2-propanol.[20] In 1:1 NH_4HCO_3/2-propanol, E7A-kB1 has a reported yield of 13%,[20] and we found here that E7D-kB1 also has a lower folding yield than the native peptide at 10%. Interestingly, the synthetic analogue D6E-kB12, in which the Glu has been reintroduced into the sequence, did not fold

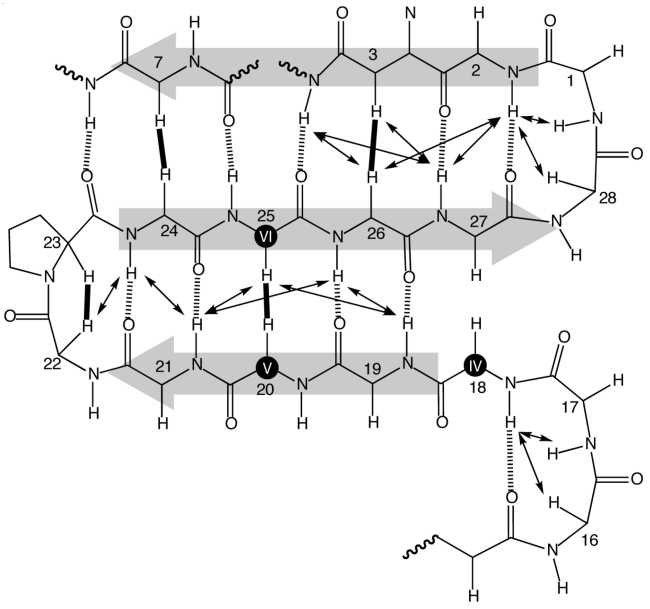

Figure 3. Secondary structure of kalata B12. To illustrate the position of the residues, three cysteines (Cys^{IV}, Cys^{V}, and Cys^{VI}) are highlighted with bold circles and the residue numbers labeled. Observed NOEs are drawn as either double-headed arrows (NH to NH NOEs or NH to αH NOEs) or thick lines (αH to αH NOEs). Predicted hydrogen bonds are also shown. The β-strands are indicated by gray arrows.

under any tested conditions. Thus, based on these folding trials, it appears that although the Glu does aid the folding of kB1, its absence is not the reason for the poor folding of kB12.

Solution Structure of kalata B12. The structure of kB12 was solved using data from homonuclear two-dimensional NMR experiments. As shown in Figure 2, the peaks in the amide region of NMR spectra recorded at pH 5.0 are well dispersed, suggesting a well-folded tertiary structure. When the pH was lowered from 5.0 to 3.0, some peaks broadened slightly, implying a degree of conformational interchange at lower pH. The other notable feature seen at both pH values was that the TOCSY peaks were very weak or undetectable at the amide frequency of Tyr22, which is connected to Pro23 via a *cis*-peptide bond that is characteristic of the Möbius subfamily. The absence of the Tyr22 TOCSY peaks was later explained by the structure of kB12, which showed that Tyr22 has an ϕ angle of $-30°$. This ϕ angle is equivalent to a dihedral angle of 90° between the NH and αH protons, giving rise to a small three-bond scalar coupling constant between the NH and αH protons, which results in poor magnetization transfer during the mixing time of the TOCSY experiment. Weak or undetectable TOCSY peaks for the residue involved in the *cis*-X-Pro peptide bond of the Möbius subfamily, due to an unusual ϕ angle, have been reported for other Möbius cyclotides, including kB1.[15]

Using the NOE, dihedral and hydrogen bond restraints, a set of structures was solved using simulated annealing. Preliminary analysis of the restraints suggested the probable presence of a triple-stranded β-sheet, as illustrated in Figure 3. A β-hairpin loop centered in loop 5 has been observed for other cyclotide structures, and a distorted third β-strand stretching through loop 1 is often reported.[36] The presence of the triple stranded β-sheet was confirmed in the final structure of kB12, as shown in Figure 4. The superimposition of the 20 lowest energy structures of kB12

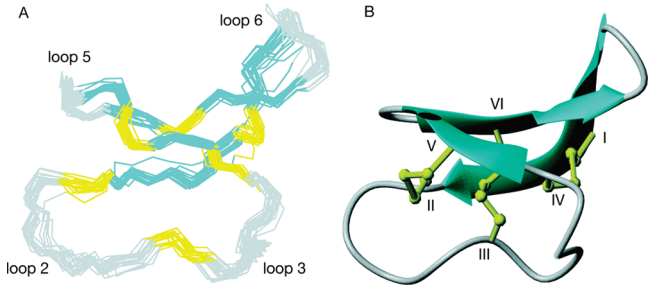

Figure 4. Structure of kalata B12. The 20 lowest energy structures are shown in panel A. Panel B shows a ribbon diagram of the solution NMR kalata B12 structure, highlighting the secondary structure and cystine knot. The loops and cysteine residues are labeled.

Table 1. Geometric and Energetic Statistics for 20 Lowest Energy Structures of kalata B12

NMR Distance and Dihedral Constraints	
Distance constraints	
total NOE	277
intraresidue	135
inter-residue	142
sequential ($\|i-j\|=1$)	95
medium-range ($\|i-j\|\leq 4$)	22
long-range ($\|i-j\|\geq 5$)	25
intermolecular	0
hydrogen bonds	9
Total dihedral angles	15
ϕ	11
χ^1	4
Structure Statistics	
Violations (mean and sd)	
distance constraints (Å)	-0.12 ± 0.08
dihedral angle constraints (°)	2.55 ± 1.69
max dihedral angle violation (°)	4.41
max distance constraint violation (Å)	−0.35
Deviations from idealized geometry	
bond lengths (Å)	0.004 ± 0.0002
bond angles (°)	0.61 ± 0.04
impropers (°)	0.49 ± 0.05
Average pairwise rmsd[a] (Å)	
backbone	0.66 ± 0.18
heavy	1.22 ± 0.26

[a] Pairwise rmsd was calculated among 20 refined structures.

gave an rmsd of 0.66 Å for the backbone and 1.22 Å for the heavy atoms. The backbone rmsd was of lower precision than that typically obtained for other cyclotide structures, suggesting a higher degree of backbone flexibility. The structural statistics, as summarized in Table 1, show that the ensemble of structures was in good agreement with the experimental restraints.

Since kB12 belongs to the Möbius subfamily of cyclotides, it was of interest to compare its structure to the prototypic Möbius cyclotide, kB1. A comparison of αH secondary chemical shifts (shown in Figure 5A), which, in general, are sensitive to the backbone topology of proteins, suggested that the variation between the structures of kB1 and kB12 was predominantly in

dx.doi.org/10.1021/bi2004153 |*Biochemistry* 2011, 50, 4077–4086

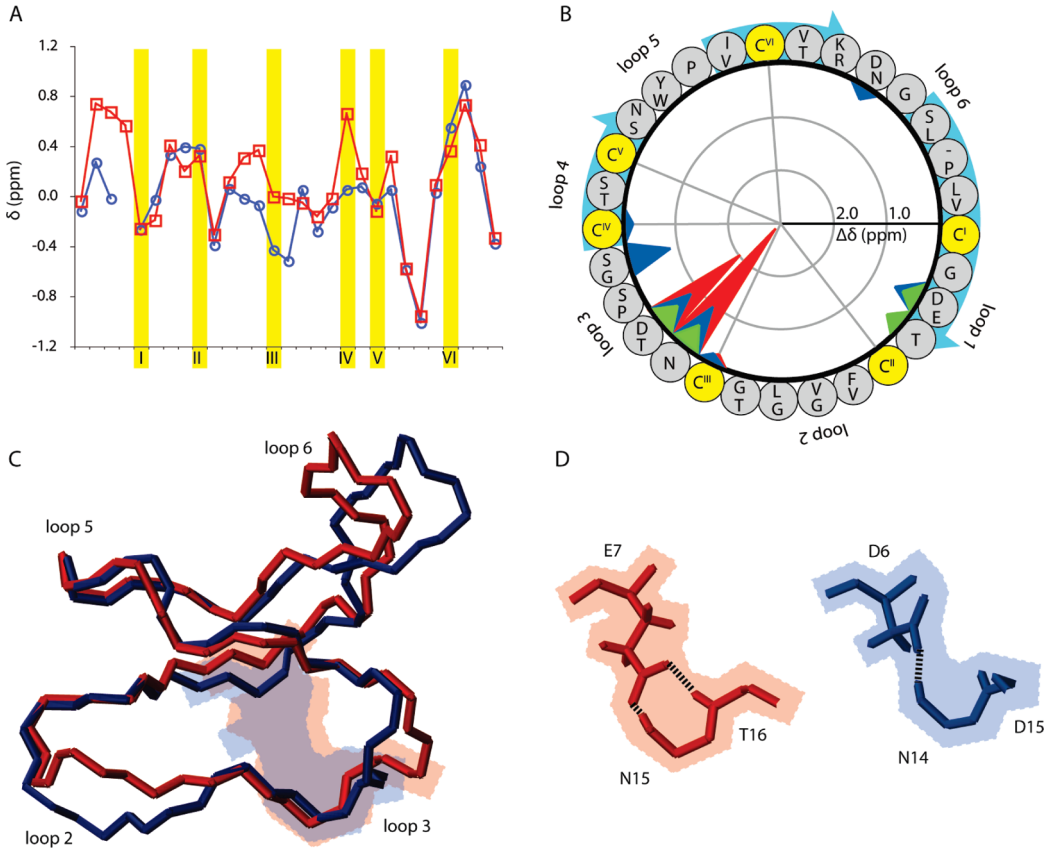

Figure 5. Comparison of kalata B1 (kB1) and kalata B12 (kB12) structures and the Glu7/Asp6 hydrogen bond network. In all panels, kB1 data are colored red, kB12 data blue, and E7D-kB1 are colored green. Panel A shows a comparison of αH secondary chemical shifts of kB1 and kB12, which were generated using random coil chemical shifts from Wishart et al.[48] Panel B shows the absolute change in NH chemical shift when the pH is varied from 3.0 to 5.0. An alignment of the structures of kB1 and kB12 is presented in panel C, where the shaded region represents the position of a hydrogen bond network involving Glu7/Asp6. The hydrogen bond network is shown in more detail in panel D. For kB1, the carboxyl of Glu7 forms hydrogen bonds with the amides of Asn15 and Thr16. For kB12, the carboxyl of Asp6 forms a hydrogen bond with Asn14.

loops 2, 3, and 6. An overlay of the structures of the two cyclotides, shown in Figure 5C, confirms that loops 2, 3, and 6 of kB12 adopt slightly different conformations than kB1. Thus, these differences reflect the differences in the loop sequences. For example, loop 6 in kB12 is one residue shorter than in kB1 and lacks a proline residue. Prolines typically cause a tight bend in protein backbones, which may explain why the conformation of loop 6 in kB12 is more extended than in kB1. In contrast, the αH secondary chemical shifts of E7D-kB1 show very little change when compared with kB1 (data not shown).

Hydrogen Bond Network. The presence of an Asp in loop 1, instead of the highly conserved Glu, is the most important feature that distinguishes kB12 from all other known cyclotides. This highly conserved Glu has been shown to form a hydrogen bond network with two residues in loop 3 in other cyclotide structures determined so far. In the structure of kB1, the side-chain carboxyl of Glu7 hydrogen bonds to the backbone amides of Asn15 and Thr16. It was of interest to see if a similar hydrogen bond network exists in the structure of kB12, that is, if Asp6 (which has a shorter side-chain relative to Glu7) hydrogen bonds to Asn14 and Asp15. Since the carboxyl groups of Asp or Glu residues are pH sensitive, the NH chemical shifts of kB12 were monitored as the pH was increased from 3.0 to 5.0, and the results were compared with those reported for kB1 [19] and E7D-kB1, as shown in Figure 5B. The change in NH chemical shifts of Asn14 and Asp15 in response to pH variation indicated that the amides of Asn14 and Asp15 were in close proximity to the carboxyl of Asp6. However, the reduced magnitude of change in NH chemical shifts relative to the respective values for Asn15 and Thr16 of kB1 suggests that the hydrogen bond network is weaker, or more transient, in kB12. A similar trend is seen in E7D-kB1.

This weaker hydrogen bond network in the structure of kB12 is apparent from Figure 5C,D, which shows that on average only one oxygen atom of the Asp6 carboxyl group can stretch over to hydrogen bond with the amide of Asn14. Despite this limitation of the shorter Asp side-chain, molecular dynamics simulations show (as discussed later) that the backbone of kB12 allows the amide of Asp14 to come into close proximity to the carboxyl of Asp6 at times to form a hydrogen bond.

The network of hydrogen bonds examined above is part of a larger network that helps stabilize the cyclotide fold. To determine any effects of the Glu residue on the overall rigidity of the cyclotide framework, the complete hydrogen bond network of kB12, kB1, and E7D-kB1 was studied by detecting slow exchanging amides and measuring amide temperature coefficients, as shown in Figure 6. With respect to amide exchange, the main differences between kB12 and kB1 were that Cys^{IV} (i.e., Cys18 in kB12; Cys19 in kB1) was slowly exchanging in kB1, but not kB12. Cys^{IV} is located at the end of loop 3, and thus the change in slow exchange behavior implies that loop 3 is slightly more

dx.doi.org/10.1021/bi2004153 |*Biochemistry* 2011, 50, 4077–4086

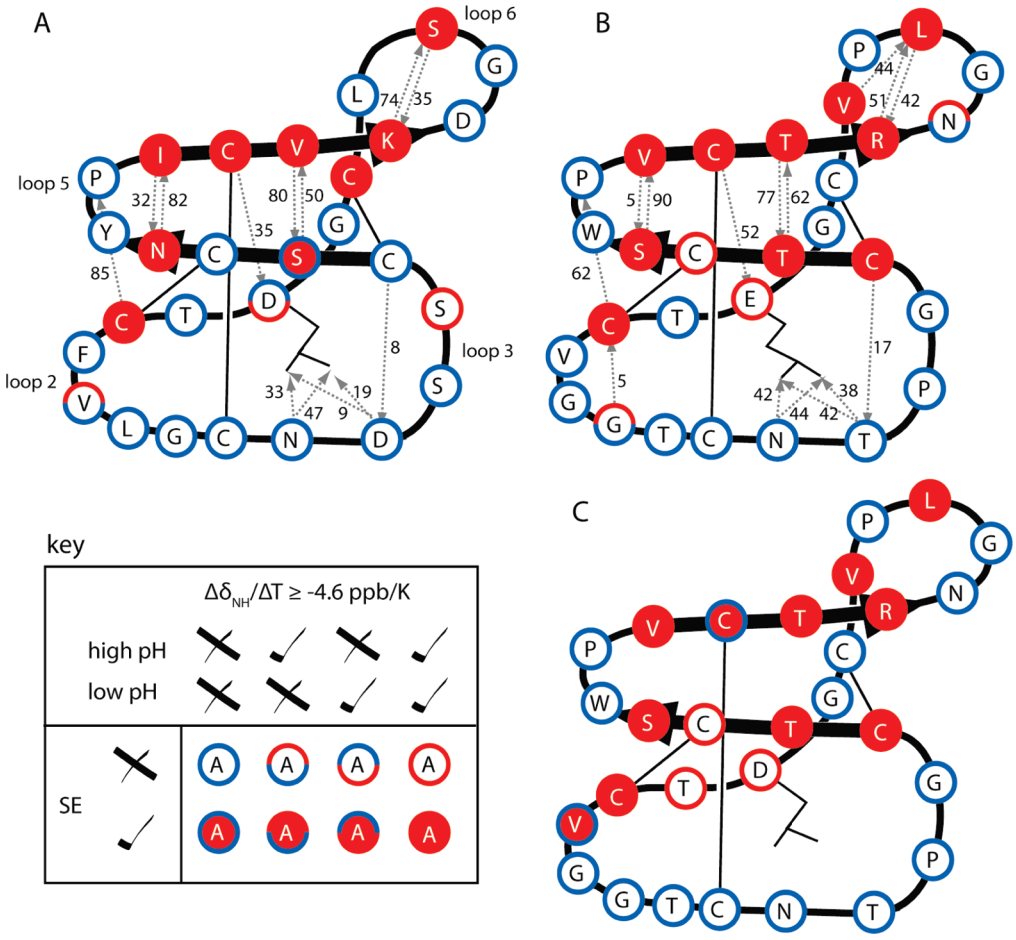

Figure 6. Hydrogen bond network of kalata B12 (kB12), kalata B1 (kB1), and E7D-kalata B1 (E7D-kB1). Each residue is drawn onto a schematic of the cyclotide backbone. Hydrogen bond properties are illustrated for kB12 (panel A), kB1 (panel B), and E7D-kB1 (panel C). A key explaining the coloring of each residue is presented in the lower left-hand corner. Different colors are used depending on whether the amide is slowly exchanging (SE) and on the value of their amide temperature coefficient. Slowly exchanging amides and amide temperature coefficients for kB1 were taken from a previous publication.[15] Molecular dynamics simulations in water were performed for kB12 and kB1 and the numbers next to each hydrogen bond in panels A and B represent the percentage occupancy observed in these simulations.

flexible in kB12. This Cys remains slow exchanging in E7D-kB1, suggesting that the difference in flexibility is more likely the result of the Pro17-Gly18 sequence in kB1 keeping the turn more ordered than the Ser16-Ser17 sequence in kB12, than the fact that Asp6 of kB12 is unable to stabilize loop 3 via hydrogen bonds as well as Glu7 of kB1.

Hydrogen bonded amides can also be detected by measuring amide temperature coefficients, that is, the sensitivity of amide chemical shifts to changes in temperature ($\Delta\delta_{NH}/\Delta T$).[37] Generally, amide temperature coefficients $\Delta\delta_{NH}/\Delta T \geq -4.6$ ppb/K indicate the presence of a hydrogen bond, whereas $\Delta\delta_{NH}/\Delta T < -4.6$ ppb/K suggest that the measured amide is accessible to solvent.[38] A comparison of the amide temperature coefficients in Figure 6 is consistent with the amide exchange data and shows no dramatic differences between the peptides, suggesting that the presence or absence of Glu does not greatly affect the overall hydrogen bond network. Ser17 in kB12 has a temperature coefficient indicative of a hydrogen bond, and analysis of the structures reveals that it interacts with the side-chain carboxyl of Asp15, which also explains the effect of pH on its chemical shift (Figure 5B). The change in temperature coefficient of Thr8 in E7D-kB1 relative to kB1 suggests subtle changes in loop 1 as a result of a reduced interaction with loop 3.

A deeper understanding of the dynamics of the hydrogen bonds was sought by calculating their percentage occupancy over a 10 ns simulation period using molecular dynamics, and the results are shown in Figure 6. In general, the most stable hydrogen bonds are part of the β-sheet secondary structure centered in loop 5, which suggests that this region of the structure is the most stable. The simulations show that hydrogen bond network involving the Glu of kB1 and the Asp of kB12 of loop 1 is relatively dynamic. For example, each oxygen atom of the Glu7 carboxyl side-chain of kB1 can switch between forming a hydrogen bond with either Asn15 or Thr16. The simulations also support the suggestion of kB12 being more flexible than kB1, as reflected for example in the much lower occupancy percentages for hydrogen bonds to the backbone of Asp15 in kB12 compared to Thr16 in kB1.

Enzymatic, Acid, and Thermal Stability. The stabilities of kB1, E7A-kB1, and kB12 were assessed by measuring their resistance to proteolysis, acid hydrolysis, and high temperature. The proteolysis studies were performed by measuring the peak intensity of analytical HPLC traces of the intact peptides over time in the presence of chymotrypsin. kB1 and E7A-kB1 have previously been shown to be completely resistant to cleavage by

dx.doi.org/10.1021/bi2004153 |*Biochemistry* 2011, 50, 4077–4086

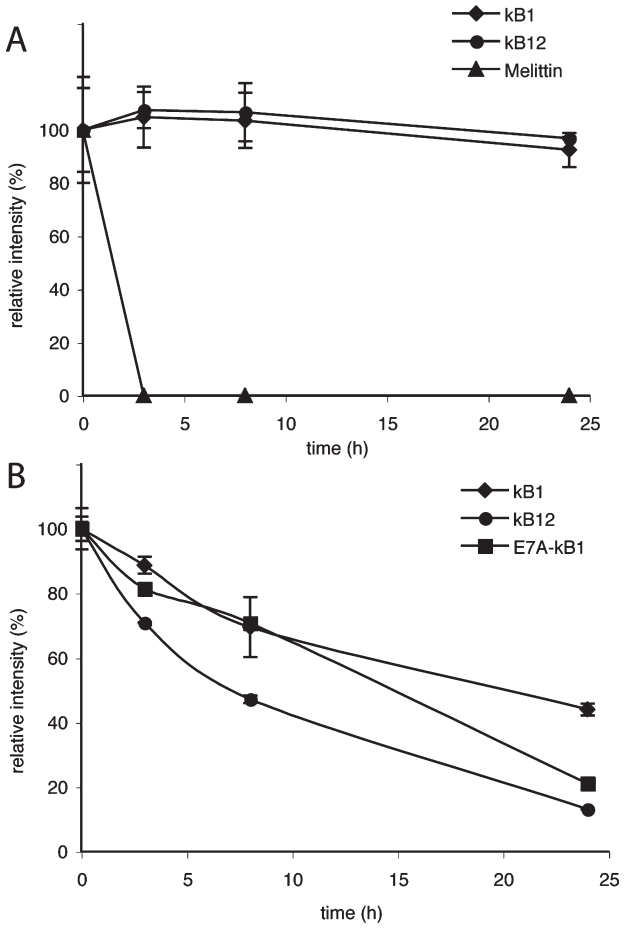

Figure 7. Results from an enzymatic stability and acid stability assays. (A) Kalata B1 (kB1) and kalata B12 (kB12) were each incubated at 37 °C with chymotrypsin and their abundances at several time-points were measured at 215 nm on an analytical RP-HPLC. Melittin was used as a positive control and degraded before the first time-point. (B) Kalata B1 (kB1), E7A-kalata B1 (E7A-kB1), and kalata B12 (kB12) were each incubated at 37 °C with HCl and their abundances at several time-points were measured at 215 nm on an analytical RP-HPLC.

various enzymes including trypsin and proteinase K.[13,20] For this study, chymotrypsin was chosen as a representative proteolytic enzyme. kB12 contains potential cleavage sites in both loop 2 and loop 6 (Leu11 and Leu3). Both kB12 and kB1 were found to be impervious to digestion by chymotrypsin (Figure 7). A linear control peptide degraded rapidly under the same conditions, with no intact peptide detected after 3 h. Acid hydrolysis experiments were conducted at 37 °C. After 24 h incubation in the presence of acid, there was 44% of kB1, 22% of E7A-kB1, and 13% of kB12 remaining, as shown in Figure 8. The observed stability of kB1 against acidic conditions agrees with a previous study,[13] but from the current study it is clear that E7A-kB1 and kB12 are less resistant to acid. Thermal stability was assessed by monitoring the 1D NMR spectra of kB12 on cycling from 25 to 80 °C and back to 25 °C. The spectra of kB12 were unchanged on return to the original temperature. Thus, it appears that the substitution of the Glu does not affect the temperature stability of cyclotides, as E7A-kB1 has been reported to maintain its global fold, as judged by 1D NMR spectra, after heating to 80 °C.[20] Overall, these assays show that the Glu substitution affects mainly the stability of cyclotides in acidic conditions.

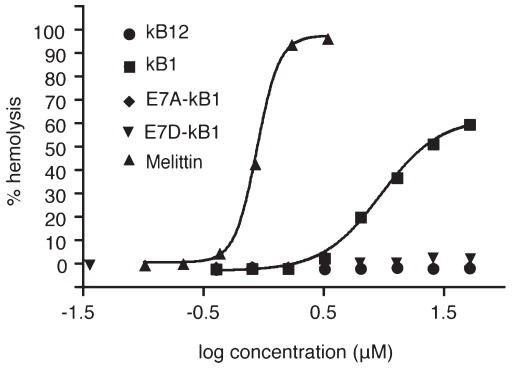

Figure 8. Hemolytic assay on selected cyclotides. Kalata B1 (kB1), E7A-kalata B1 (E7A-kB1), E7D-kalata B1 (E7D-kB1), and kalata B12 (kB12) were incubated with human red blood cells and the percentage hemolysis was measured at different time-points. Both E7A-kB1 and kB12 showed negligible hemolytic activity.

Hemolytic Activity. The biological activity of kB12 was assessed in a hemolytic assay, which is typically used as a marker of cyclotide activity because they are believed to act through membrane disruption. The positive controls of melittin and kB1 showed activities similar to those reported in previous studies, with 1.7 μM of melittin and 16 μM of kB1 causing 50% hemolysis of human red blood cells.[20] Interestingly, kB12, E7A-kB1, and E7D-kB1 all had almost negligible hemolytic activity, as shown in Figure 8, which indicates the replacement of the Glu significantly affects cyclotide bioactivity, most likely by modulating how cyclotides interact with membranes, since membrane binding is a prerequisite of hemolytic activity.

DISCUSSION

Cyclotides are a family of natural insecticidal peptides with remarkable stability and tolerance to residue substitution, which gives them exciting potential to be developed as protein engineering scaffolds for a variety of agricultural and pharmaceutical applications.[36,39] Analysis of all known cyclotide sequences shows that a Glu in loop 1 is the most highly conserved noncysteine residue and is believed to contribute to the stability and activity of cyclotides. Here we characterized the folding, structure, stability, and activity of kB12, the only naturally occurring cyclotide without the conserved Glu in loop 1. We compared these results to those obtained for the prototypical cyclotide, kB1, and two mutants, E7A-kB1 and E7D-kB1, and showed that the presence of a Glu residue in loop 1 has a role in the stabilization of the overall cyclotide fold, influences the flexibility of loop 3, and modulates the membrane-disrupting activity of cyclotides. These findings have potential significance in drug design applications of the CCK protein engineering scaffold and are important for enhancing our understanding of the mechanism of action of cyclotides.

The impact of the Glu to Asp substitution in loop 1 was determined by solving the structure of kB12 in solution using NMR spectroscopy. Given the exceptionally high conservation of the Glu, it was surprising to find that kB12 adopts an almost identical overall fold to kB1 as well as other cyclotide structures determined so far. A β-hairpin, comprising two β-strands centered in loop 5, is the secondary structure element common to all cyclotides that have been structurally characterized so far and is also present in the structure of kB12. A third β-strand, made up of

segments of loops 1 and 6, is distorted in some cyclotides, including kB1, but is well-defined in kB12. Tricyclon A (whose sequence is shown in Figure 1) is another example of a cyclotide that has a well-defined triple-stranded β-sheet.[40] The main conclusion that can be drawn from the structural studies reported here is that the conserved Glu appears not to be essential for *defining* the CCK fold; rather, the fold appears to be determined mainly by the spacing and connectivity of the six conserved Cys residues. The ability of cyclotides to maintain a similar overall fold regardless of sequence variations at non-cysteine positions, including at the highly conserved Glu, confirms that the CCK motif is a robust framework and is thus suitable for protein engineering studies.

Although the conserved Glu apparently is not critical for *defining* the shape of the CCK structure, it does seem to have a role in *increasing folding yields* of cyclotides and in *stabilizing* the structures once formed; that is, it assists in the process of folding the structure to its final shape, and then keeping it there. The mechanism by which the Glu residue facilitates folding is not known but presumably involves stabilization (via hydrogen bonding) of key intermediates in the folding pathway. To our surprise, the attempted introduction of a Glu instead of the naturally occurring Asp in kB12 did not improve in vitro folding but rather prevented correct folding of the D6E-kB12 mutant. This suggests that in the case of kB12 other sequence changes compensate for the missing natural Glu seen in all other cyclotides, making an Asp the preferred residue at this position. Although our studies monitored the in vitro folding process, the strong conservation of the Glu residue in 159 of 160 reported naturally occurring cyclotides supports an important role for it in the in planta folding pathway. Consistent with this proposal is the observation that kB12, which lacks the conserved Glu and folds poorly in vitro, is one of the least abundant of the 17 cyclotides reported so far[22] in *O. affinis*, the plant in which cyclotides were originally discovered. As far as a role in structural stabilization is concerned, in previously characterized cyclotides the Glu residue is believed to help stabilize the CCK framework by participating in a hydrogen bond network with the backbone amides of two residues in loop 3. A similar network is present in kB12, but compared to a Glu, the shorter side-chain of Asp reduces the strength (and occupancy) of the hydrogen bond network, which in turn reduces the rigidity of loop 3 in particular. Thus, the current study confirms a role for the conserved Glu in stabilizing cyclotides by rigidifying them via hydrogen bond formation.

To further explore the importance of Glu in the stability of cyclotides, enzyme digestion, acid hydrolysis, and temperature assays were carried out. These studies showed that the absence of a Glu in loop 1 does not significantly affect the stability of cyclotides against proteolytic enzymes or high temperature. This finding confirms that the presence of the CCK motif, that is, the circular backbone and a disulfide knot, is a strong stabilizing structural feature. However, the lack of a Glu residue reduces the stability of cyclotides to acidic conditions. Overall, the results suggest that a complementary array of structural features contribute to cyclotide stability, some important to thermal stability or susceptibility to proteolysis, and others important to chemical stability.

We also examined the role of the highly conserved Glu in biological activity of cyclotides. Hemolytic assays were used to test the activity of kB12, kB1, E7D-kB1, and E7A-kB1, as cyclotides are believed to deliver their activity through membrane interactions.[3,41,42] The assay results showed that substitution of the Glu with either Asp or Ala resulted in loss of hemolytic activity relative to kB1. Masking of the charge of the Glu through methylation of cycloviolacin O2, a bracelet cyclotide, has also been shown to result in a loss of cytotoxic activity.[21] Overall, it is clear that the Glu in loop 1 is critical for the biological activity of cyclotides. Both the presence and the location of the charge are important for biological activity as evidenced by the lack of hemolytic activity despite the presence of a negative charge in E7D-kB1. Previous studies had addressed only the presence/absence of the charge of the Glu residue via mutagenesis or chemical modification, but the results here clearly show that the location of the side-chain carboxyl group appears to be critical for activity. This finding suggests that the Glu is involved in a specific interaction, either intra- or intermolecular, that mediates cyclotide activity, rather than just providing a site of negative charge. Such an interaction might modulate the broad mechanism of action proposed for cyclotides, namely, interactions with membranes via their surface patch of hydrophobic residues.[20]

The hemolytic activity of cyclotides has been reported to be dependent on their surface hydrophobicity; cyclotides with larger hydrophobic surface areas have increased hemolytic activities.[8,43] A larger hydrophobic surface area in principle helps the interaction of a cyclotide with the hydrophobic lipids of target membranes. Since all three cyclotides examined in this study have similar hydrophobic surface areas, the loss of activity from the replacement of the Glu strongly supports the suggestion that the Glu mediates other more specific interactions that contribute to the activity of cyclotides. One possibility is that the Glu has a role in metal-binding;[44,45] however, in an Ala scan study of kB1, a relationship between metal binding and activity could not be established because an inactive Ala mutant was still shown to bind metal ions.[20] A more likely possibility is that the Glu might facilitate the self-association of cyclotides, a process that is probably required to cause membrane disruption. Consistent with the self-association hypothesis, the cyclotide kalata B2 has been shown to form oligomers in analytical ultracentrifugation experiments,[46] and electrophysiology experiments have shown the formation of pores in membranes that are much larger than individual cyclotides.[47] The Glu may also play a role in the direct interaction with membrane lipids, either in an initial recognition step or during the pore formation process. At this stage, the precise role, if any, of the Glu residue in promoting self-association is not known.

In summary, we studied the importance of a highly conserved Glu residue in cyclotides by comparing the folding, structure, stability, and activity of kB12 with E7A-kB1, E7D-kB1, and kB1. We have shown that the overall cyclotide fold is robust and stable, which is attributed to the CCK motif and does not depend on the presence of the conserved Glu in loop 1. The Glu enhances the stability of cyclotides under acidic conditions but, more importantly, is vital for their activity, probably playing a key role in mediating cyclotide self-association. These findings are relevant to drug design or protein engineering applications based on the CCK scaffold because we now know that the hemolytic activity of cyclotides can be modulated even with the relatively conservative substitution of the Glu to an Asp.

AUTHOR INFORMATION

Corresponding Author

*Tel: 61-7-33462019; fax 61-7-33462101; e-mail: d.craik@imb.uq.edu.au

Funding Sources

This research was funded by the Australian Research Council (Grant DP0984955) and the National Health and Medical

Research Council. R.J.C. is a NHMRC CDA Fellow. KJ.R. is a UQ Postdoctoral Research Fellow. D.J.C. is a NHMRC Professorial Fellow.

■ ACKNOWLEDGMENT

We thank Ms. Yen-Hua Huang for help with synthesis; Ms. Prascilla Tagore and Mr. Jonas Jensen for help with HF cleavage; Dr. Greg Pierens for help with use of the 900 MHz spectrometer; and Kathryn Greenwood for performing the hemolytic assay on kB12. We are grateful for access to the 900 MHz NMR spectrometer of the Queensland NMR Network.

■ ABBREVIATIONS USED

CCK, cyclic cystine knot; kB1, kalata B1; kB12, kalata B12

■ REFERENCES

(1) Craik, D. J., Daly, N. L., Bond, T., and Waine, C. (1999) Plant cyclotides: A unique family of cyclic and knotted proteins that defines the cyclic cystine knot structural motif. *J. Mol. Biol. 294*, 1327–1336.

(2) Jennings, C., West, J., Waine, C., Craik, D., and Anderson, M. (2001) Biosynthesis and insecticidal properties of plant cyclotides: the cyclic knotted proteins from *Oldenlandia affinis*. *Proc. Natl. Acad. Sci. U. S. A. 98*, 10614–10619.

(3) Barbeta, B. L., Marshall, A. T., Gillon, A. D., Craik, D. J., and Anderson, M. A. (2008) Plant cyclotides disrupt epithelial cells in the midgut of lepidopteran larvae. *Proc. Natl. Acad. Sci. U. S. A. 105*, 1221–1225.

(4) Jennings, C. V., Rosengren, K. J., Daly, N. L., Plan, M., Stevens, J., Scanlon, M. J., Waine, C., Norman, D. G., Anderson, M. A., and Craik, D. J. (2005) Isolation, solution structure, and insecticidal activity of kalata B2, a circular protein with a twist: do Mobius strips exist in nature?. *Biochemistry 44*, 851–860.

(5) Gruber, C. W., Cemazar, M., Anderson, M. A., and Craik, D. J. (2007) Insecticidal plant cyclotides and related cystine knot toxins. *Toxicon 49*, 561–575.

(6) Gran, L. (1973) Isolation of oxytocic peptides from *Oldenlandia affinis* by solvent extraction of tetraphenylborate complexes and chromatography on sephadex LH-20. *Lloydia 36*, 207–208.

(7) Gustafson, K. R., McKee, T. C., and Bokesch, H. R. (2004) Anti-HIV cyclotides. *Curr. Protein Pept. Sci. 5*, 331–340.

(8) Wang, C. K., Colgrave, M. L., Gustafson, K. R., Ireland, D. C., Göransson, U., and Craik, D. J. (2008) Anti-HIV cyclotides from the Chinese medicinal herb *Viola yedoensis*. *J. Nat. Prod. 71*, 47–52.

(9) Tam, J. P., Lu, Y. A., Yang, J. L., and Chiu, K. W. (1999) An unusual structural motif of antimicrobial peptides containing end-to-end macrocycle and cystine-knot disulfides. *Proc. Natl. Acad. Sci. U. S. A. 96*, 8913–8918.

(10) Svangård, E., Göransson, U., Hocaoglu, Z., Gullbo, J., Larsson, R., Claeson, P., and Bohlin, L. (2004) Cytotoxic cyclotides from *Viola tricolor*. *J. Nat. Prod. 67*, 144–147.

(11) Witherup, K. M., Bogusky, M. J., Anderson, P. S., Ramjit, H., Ransom, R. W., Wood, T., and Sardana, M. (1994) Cyclopsychotride A, a biologically active, 31-residue cyclic peptide isolated from *Psychotria longipes*. *J. Nat. Prod. 57*, 1619–1625.

(12) Plan, M. R., Saska, I., Cagauan, A. G., and Craik, D. J. (2008) Backbone cyclised peptides from plants show molluscicidal activity against the rice pest *Pomacea canaliculata* (golden apple snail). *J. Agric. Food Chem. 56*, 5237–5241.

(13) Colgrave, M. L., and Craik, D. J. (2004) Thermal, chemical, and enzymatic stability of the cyclotide kalata B1: the importance of the cyclic cystine knot. *Biochemistry 43*, 5965–5975.

(14) Craik, D. J., Simonsen, S., and Daly, N. L. (2002) The cyclotides: novel macrocyclic peptides as scaffolds in drug design. *Curr. Opin. Drug Discovery Devel. 5*, 251–260.

(15) Saether, O., Craik, D. J., Campbell, I. D., Sletten, K., Juul, J., and Norman, D. G. (1995) Elucidation of the primary and three-dimensional structure of the uterotonic polypeptide kalata B1. *Biochemistry 34*, 4147–4158.

(16) Wang, C. K., Kaas, Q., Chiche, L., and Craik, D. J. (2008) CyBase: a database of cyclic protein sequences and structures, with applications in protein discovery and engineering. *Nucleic Acids Res. 36*, D206–210.

(17) Simonsen, S. M., Sando, L., Ireland, D. C., Colgrave, M. L., Bharathi, R., Göransson, U., and Craik, D. J. (2005) A continent of plant defense peptide diversity: cyclotides in Australian *Hybanthus* (*Violaceae*). *Plant Cell 17*, 3176–3189.

(18) Gran, L. (1973) On the effect of a polypeptide isolated from "Kalata-Kalata" (*Oldenlandia affinis* DC) on the oestrogen dominated uterus. *Acta Pharmacol. Toxicol. 33*, 400–408.

(19) Rosengren, K. J., Daly, N. L., Plan, M. R., Waine, C., and Craik, D. J. (2003) Twists, knots, and rings in proteins. Structural definition of the cyclotide framework. *J. Biol. Chem. 278*, 8606–8616.

(20) Simonsen, S. M., Sando, L., Rosengren, K. J., Wang, C. K., Colgrave, M. L., Daly, N. L., and Craik, D. J. (2008) Alanine scanning mutagenesis of the prototypic cyclotide reveals a cluster of residues essential for bioactivity. *J. Biol. Chem. 283*, 9805–9813.

(21) Herrmann, A., Svangård, E., Claeson, P., Gullbo, J., Bohlin, L., and Göransson, U. (2006) Key role of glutamic acid for the cytotoxic activity of the cyclotide cycloviolacin O2. *Cell. Mol. Life Sci. 63*, 235–245.

(22) Plan, M. R. R., Göransson, U., Clark, R. J., Daly, N. L., Colgrave, M. L., and Craik, D. J. (2007) The cyclotide fingerprint in *Oldenlandia affinis*: elucidation of chemically modified, linear and novel macrocyclic peptides. *ChemBiochem 8*, 1001–1011.

(23) Cemazar, M., and Craik, D. J. (2007) Microwave-assisted Boc-solid phase peptide synthesis of cyclic cysteine-rich peptides. *J. Pept. Sci. 14*, 683–689.

(24) Tam, J. P., and Lu, Y.-A. (1997) Synthesis of large cyclic cystine-knot peptide by orthogonal coupling strategy using unprotected peptide precursors. *Tetrahedron Lett. 38*, 5599–5602.

(25) Marion, D., and Wüthrich, K. (1983) Application of phase sensitive two-dimensional correlated spectroscopy (COSY) for measurements of ^{1}H-^{1}H spin-spin coupling constants in proteins. *Biochem. Biophys. Res. Commun. 113*, 967–974.

(26) Braunschweiler, L., and Ernst, R. R. (1983) Coherence transfer by isotropic mixing: application to proton correlation spectroscopy. *J. Magn. Reson. 53*, 521–528.

(27) Jeener, J., Meier, B. H., Bachmann, P., and Ernst, R. R. (1979) Investigation of exchange processes by two-dimensional NMR spectroscopy. *J. Chem. Phys. 71*, 4546–4553.

(28) Griesinger, C., Sørensen, O. W., and Ernst, R. R. (1987) Practical aspects of the E.COSY technique, measurement of scalar spin-spin coupling constants in peptides. *J. Magn. Reson. 75*, 474–492.

(29) Piotto, M., Saudek, V., and Sklenar, V. (1992) Gradient-tailored excitation for single-quantum NMR spectroscopy of aqueous solutions. *J. Biomol. NMR 2*, 661–665.

(30) Brünger, A. T., Adams, P. D., and Rice, L. M. (1997) New applications of simulated annealing in X-ray crystallography and solution NMR. *Structure 5*, 325–336.

(31) Koradi, R., Billeter, M., and Wüthrich, K. (1996) MOLMOL: a program for display and analysis of macromolecular structures. *J. Mol. Graph. 14*, 29–32.

(32) Laskowski, R. A., Rullmannn, J. A., MacArthur, M. W., Kaptein, R., and Thornton, J. M. (1996) AQUA and PROCHECK-NMR: programs for checking the quality of protein structures solved by NMR. *J. Biomol. NMR 8*, 477–486.

(33) Tam, J. P., Lu, Y.-A., and Yu, Q. (1999) Thia-zip reaction for synthesis of large cyclic peptides: Mechanisms and applications. *J. Am. Chem. Soc. 121*, 4316–4324.

(34) Daly, N. L., Love, S., Alewood, P. F., and Craik, D. J. (1999) Chemical synthesis and folding pathways of large cyclic polypeptides: studies of the cystine knot polypeptide kalata B1. *Biochemistry 38*, 10606–10614.

(35) Dawson, P. E., Muir, T. W., Clark-Lewis, I., and Kent, S. B. (1994) Synthesis of proteins by native chemical ligation. *Science 266*, 776–779.

(36) Craik, D. J., Cemazar, M., Wang, C. K., and Daly, N. L. (2006) The cyclotide family of circular miniproteins: nature's combinatorial peptide template. *Biopolymers 84*, 250–266.

(37) Cierpicki, T., and Otlewski, J. (2001) Amide proton temperature coefficients as hydrogen bond indicators in proteins. *J. Biomol. NMR 21*, 249–261.

(38) Wang, C. K. L., Hu, S-H., Martin, J. L., Sjogren, T, Hajdu, J., Bohlin, L., Claeson, P., Goransson, U, Rosengren, K. J., Tang, J, Tan, N-H, and Craik, D. J. (2009) Combined X-ray and NMR analysis of the stability of the cyclotide cystine knot fold that underpins its insecticidal activity. *J. Biol. Chem. 284*, 10672–10683.

(39) Clark, R. J., Daly, N. L., and Craik, D. J. (2006) Structural plasticity of the cyclic-cystine-knot framework: implications for biological activity and drug design. *Biochem. J. 394*, 85–93.

(40) Mulvenna, J. P., Foley, F. M., and Craik, D. J. (2005) Discovery, structural determination and putative processing of the precursor protein that produces the cyclic trypsin inhibitor SFTI-1. *J. Biol. Chem. 280*, 32245–32253.

(41) Svangård, E., Burman, R., Gunasekera, S., Lövborg, H., Gullbo, J., and Göransson, U. (2007) Mechanism of action of cytotoxic cyclotides: cycloviolacin O2 disrupts lipid membranes. *J. Nat. Prod. 70*, 643–647.

(42) Kamimori, H., Hall, K., Craik, D. J., and Aguilar, M. I. (2005) Studies on the membrane interactions of the cyclotides kalata B1 and kalata B6 on model membrane systems by surface plasmon resonance. *Anal. Biochem. 337*, 149–153.

(43) Chen, B., Colgrave, M. L., Wang, C., and Craik, D. J. (2006) Cycloviolacin H4, a hydrophobic cyclotide from *Viola hederaceae*. *J. Nat. Prod. 69*, 23–28.

(44) Shenkarev, Z. O., Nadezhdin, K. D., Sobol, V. A., Sobol, A. G., Skjeldal, L., and Arseniev, A. S. (2006) Conformation and mode of membrane interaction in cyclotides. Spatial structure of kalata B1 bound to a dodecylphosphocholine micelle. *FEBS J. 273*, 2658–2672.

(45) Skjeldal, L., Gran, L., Sletten, K., and Volkman, B. F. (2002) Refined structure and metal binding site of the kalata B1 peptide. *Arch. Biochem. Biophys. 399*, 142–148.

(46) Nourse, A., Trabi, M., Daly, N. L., and Craik, D. J. (2004) A comparison of the self-association behavior of the plant cyclotides kalata B1 and kalata B2 via analytical ultracentrifugation. *J. Biol. Chem. 279*, 562–570.

(47) Huang, Y. H., Colgrave, M. L., Daly, N. L., Keleshian, A., Martinac, B., and Craik, D. J. (2009) *J. Biol. Chem. 284*, 20699–20707.

(48) Wishart, D. S., Bigam, C. G., Holm, A., Hodges, R. S., and Sykes, B. D. (1995) ^{1}H, ^{13}C and ^{15}N random coil NMR chemical shifts of the common amino acids. I. Investigations of nearest-neighbor effects. *J. Biomol. NMR 5*, 67–81.